frontiers | Frontiers in Materials

TYPE Original Research
PUBLISHED 01 June 2023
DOI 10.3389/fmats.2023.1209186



OPEN ACCESS

EDITED BY
Guo-Bin Ding,
Shanxi University, China

REVIEWED BY
Na Shen,
Chinese Academy of Sciences (CAS), China
Di Huang,
Taiyuan University of Technology, China

*CORRESPONDENCE
Yuan Yao,
yaoyuan_cq@hotmail.com

RECEIVED 20 April 2023
ACCEPTED 23 May 2023
PUBLISHED 01 June 2023

CITATION
Yao Y, Gao X and Zhou Z (2023), The application of drug loading and drug release characteristics of two-dimensional nanocarriers for targeted treatment of leukemia.
*Front. Mater.* 10:1209186.
doi: 10.3389/fmats.2023.1209186



# The application of drug loading and drug release characteristics of two-dimensional nanocarriers for targeted treatment of leukemia

Yuan Yao*, Xiaoli Gao and Zaifu Zhou

Chongqing Chemical Industry Vocational College, Chongqing, China

The development of bioinformatics technology has enabled nanomedicine to play a significant role in drug delivery systems. Its low toxicity, high efficiency, and controllable drug release advantages make it have good application effects. Moreover, common targeted therapeutic drug formulations have weak stability in malignant tumor leukemia, and their application effects are limited. Therefore, based on the characteristics of black phosphorus two-dimensional nanomedicine, experimental designs were conducted on its nanosheet preparation, polyethylene glycol modification, and anti-tumor drug loading. Experimental analysis was also conducted on the characterization ability, drug release, and targeted therapy of nanomedicine. The results show that polyethylene glycol (PEG) modified black phosphorus crystals (BP) nanoparticles can effectively improve their negative electricity, and have relatively stable photothermal properties. The release of doxorubicin hydrochloride (DOX) loaded nanoparticles was analyzed. It was found that the maximum drug release efficiency of BP-PEG-DOX was higher than that of BP-DOX at pH 5 and 7.5 (12.13% > 7.69%, 29.46% > 28.69%). The maximum drug release rates of BP-PEG-DOX-NIR reached 33.23% and 28.67% at temperatures of 35°C and 45°C, with differences of over 10% compared to the non laser group. Moreover, the nano drug loaded particles modified with PEG and treated with laser have a significant killing effect on cells, with a decrease in cell survival rate of over 15%. The two-dimensional nano drug carrier has high safety and effectiveness in drug delivery, and its targeted treatment effect on acute T lymphoblastic leukemia cells is obvious. Its drug release characteristics perform well in photothermal therapy, indicating that black phosphorus nano drugs can improve the biological safety and applicability of drugs in new tumor targeted therapy.

KEYWORDS

**two-dimensional nanomedicine, drug loading, drug release rate, black phosphorus, leukemia, targeted treatment**

## 1 Introduction

Leukemia is a malignant tumor of the hematopoietic system, mainly characterized by cell deoxyribonucleic acid mutations. It causes malignant proliferation of hematopoietic stem cells in the bone marrow, resulting in the production of cancerous cells that lack normal physiological functions. It can also infiltrate other non-hematopoietic tissues and organs, inhibiting normal hematopoiesis in severe cases. According to the severity of its course and its cell differentiation, leukemia can be divided into acute leukemia, which grows rapidly and

has a shorter course, and chronic leukemia, which progresses slowly and has a longer duration (Medina-Sánchez et al., 2018; Zhang et al., 2020). Currently, clinical treatment methods for leukemia include chemotherapy, radiation therapy, cell transplantation, and targeted therapy. Chemoradiotherapy kills cancer cells through the intake of chemotherapy drugs and radiation therapy, but the side effects are significant, causing damage to normal tissues and the immune system, with varying results for different patients (Guo et al., 2018). Cell transplantation rebuilds normal immune function by repairing or replacing damaged cells, but the presence of residual cancer cells in the transplanted tissue and the susceptibility to complications affecting the patient's quality of life (Moller and Bein, 2019; Liu et al., 2019; El-Boubbou, 2018a). Targeted therapy uses targeted drugs to maintain a high concentration of the drug in the tumor area, improving the killing efficiency of cancer cells while avoiding damage to other normal cells. Its specificity for cancerous sites ensures its effectiveness while maintaining safety. However, the targeting and stability of conventional drug formulations such as modified nanoparticles, microspheres, liposomes, and prodrugs are weak, and finding effective drug delivery methods is an important research topic (Kimura et al., 2018; Rai et al., 2018). The emergence of genomics in the 2000s generated a large number of databases and computational tools, which were analyzed through bioinformatics to obtain valuable information about the regulation of different organisms' genomes. Drug delivery systems seem to be a new method for improving drug targeting and release into cells, bringing new opportunities for improving drug efficiency and avoiding potential side effects. The relationship between target discovery, drug discovery, and drug delivery, as well as their computational strategies, is closely related to the development of the medical field. Duarte, Y scholar, conducted a needs analysis and related improvements in the field of bioinformatics and medical drug delivery in their review. Developing multifunctional nanocarriers with stimulus responsive drug release control capabilities can address many challenges in current cancer treatment (Duarte et al., 2019). Nanomaterials have good biocompatibility and no obvious toxicity when used for drug loading. And the consistency between the MTT analysis data of scholars Paknia and F and the bioinformatics predictions is consistent. For the first time, new functional nanocarriers have good application effects in the delivery of anticancer drugs and targeted cancer treatment (Paknia et al., 2022). The progress and development of bio-medicine has highlighted the advantages of nanomaterials in the fields of bio-imaging and drug delivery. Nanomaterials refer to materials composed of nano-scale structural units or those with at least one location in the nano-scale range in three-dimensional space, demonstrating good surface effects and size effects. Nanodrug carriers in the field of bio-medicine primarily employ diffusion, absorption, or covalent binding to load therapeutic drugs, better releasing drug efficacy in the blood to achieve the intervention effect of killing cancer cells. This nano-drug loading approach can improve targeting aggregation at the target site, improve the solubility and absorption rate of poorly soluble drugs, and mitigate drug side effects through its good sealing properties (El-Boubbou, 2018b; Li et al., 2019). Common types of nanocarriers include organic ones (such as polymers, lipids, and carbon-based materials) and inorganic ones (such as magnetic, noble metal, and semiconductor nanoparticles), with physical or chemical stimuli being the response conditions for evaluating controlled drug release, and targeting being a key manifestation of nanodrug carriers (Dadwal et al., 2018; Zong et al., 2019a; Cai et al., 2019). Black phosphorus (BP), as a non-metallic layered semiconductor, has a primarily folded layered scale structure, which can be peeled into single or multi-layer two-dimensional nanosheets. Its broad absorption spectra range exhibits good photothermal conversion efficiency, making it commonly applied in photodynamic therapy. BP does not produce toxic by-products during oxidation and has good biocompatibility as an inorganic material (Pullan et al., 2019; Jin et al., 2020). Most researchers pay more attention to the preparation of BP nanosheets, nanocomposite materials, and their application to photothermal therapy. There is limited research on the application of BP in drug delivery systems and leukemia treatment. Therefore, analyzing the drug loading, drug release characteristics, and targeted therapeutic effects of two-dimensional nanodrug BP may provide references for advancing material preparation and targeted therapy research processes.

# 2 Drug loading and drug release characteristics of two-dimensional nanocarriers in targeted treatment of leukemia

## 2.1 Experimental design for the preparation of two-dimensional nanodrug BP

### 2.1.1 Experimental materials, reagents, and instruments

BP was purchased from a certain technology company and stored in a cool, ventilated place, and due to its easy oxidation, BP needs to be stored in a glove box filled with argon gas. Argon gas, as an inert gas, exhibits good stability. Polyethylene glycol ($NH_2HCl$-PEG2000-$NH_2HCl$, PEG) was purchased from a certain biological company. Modified BP with PEG has a longer shelf life, effectively avoiding its degree of oxidation and degradation, and improving its stability and aggregation. The raw materials used in the experiment, cell culture medium, CCK-8 cell proliferation assay kit, calcein-AM, and cell detection reagents were selected from a certain biotechnology company. 1-ethyl-carbodiimide hydrochloride and N-hydroxysuccinimide were purchased from a certain chemical company. The Sgc8 aptamer (Sequence: 5′COOH-ATCTAACTGCTGCGCCGCCGGGAAAATACTGATCGGTTAGA-3′) was synthesized by a certain biotechnology company (Shao et al., 2021). At the same time, the human acute lymphatic leukemia cells (CCRF-CEM) used in the study were purchased from the cell bank of the Institute of Life Sciences, Chinese Academy of Sciences. The instruments used in the experiment include an ultrasonic pulverizer with frequency of 19–23 Hz and controllable temperature. The model is Tecnai G2T20, with a voltage and resolution of 20-200 KV and 0.19 nm. It is a transmission electron microscope that can perform sample morphology analysis and energy spectrum composition analysis. ZEN3690 potential analyzer is used. A UV spectrophotometer with a model of UV-3600 PC that can analyze the absorption spectrum

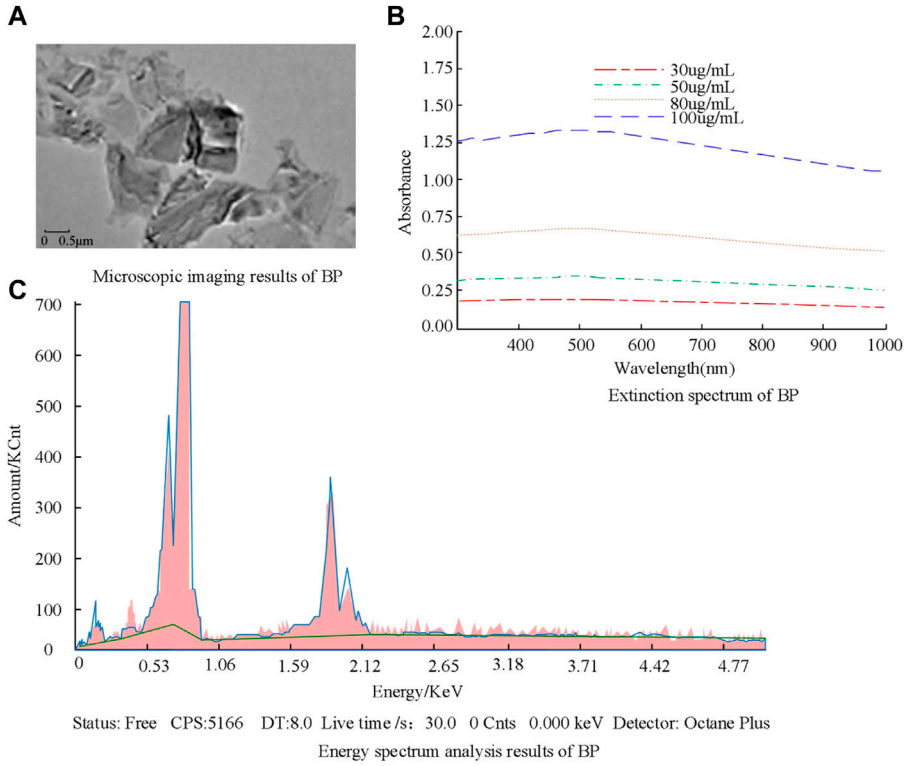


FIGURE 1
BP morphology and spectral absorption.

characterization of samples is adopted. The model is Mira Model 900-F, which uses pulsed femtosecond lasers and femtosecond lasers with wavelengths of 200 and 808 nm. FV1000 laser microscope and 96 well enzyme-linked immunosorbent assay are adopted. There are other basic experimental instruments (test tubes, heating stirrers, thermometers, measuring cylinders, straws, scales, drying ovens, centrifuges, dialysis bags, cell culture dishes, cleaning machines, etc.) (Kong et al., 2020; Herrmann et al., 2021; Zhu et al., 2021).

### 2.1.2 Design of BP nanoparticle preparation and related test performance methods

The block-shaped BP crystal is taken out and ground in an agate mortar for 30 min, and 25 mg of BP powder is weighed using an electronic balance for experimental preparation. The BP powder is placed in deionized water (18 $M\Omega^{-1}$) that has been previously depleted of dissolved oxygen. Then, ultrasonic homogenizer is used to act on the solvent mixed with BP powder and deionized water to destroy the van der Waals force between BP and achieve exfoliation. Ultrasonic homogenization is achieved by using ultrasonic waves to release the energy of the bubbles in solution during the disruption process, generating high pressure and temperature to separate BP nanosheets (Qiu et al., 2018). The pre-temperature of the ultrasonic homogenizer should be below 4°C, and the distance between the probe and the bottom of the glass container should be greater than 1 cm. The ultrasonic period and duration are 7 s and 12 s, respectively, with the power set to 900 W. It can be observed that the color of BP crystals turns dark brown after grinding. The BP solution is then centrifuged at 1,500 rpm for 15 min to obtain a clear dispersion liquid (Liu et al., 2021; Wang et al., 2021). The clear dispersion liquid is then subjected to a second centrifugation at a speed and time of 7,800 rpm and 25 min, respectively, to obtain treated BP, which is stored in deoxygenated water and low-temperature drying oven for experimental use. Thus, the preparation of BP nanosheets is completed. For PEG modification of BP, a sample of 10 mg and 10 ml is used, and the mixed solution is subjected to ultrasonic treatment for 30 min and stirred to dissolve. The operation of the second centrifugation is the same as above. If there is excess PEG during the process, it needs to be cleaned by deionized water.

Performance testing of BP: 30 μl of the prepared BP solution is added to 1 mL of deionized water and shaken well. The treated test solution is then placed in the sample cell for analysis using a potentiostat. For spectral measurements, BP solutions of 30, 50, 80, and 100 μg/mL are prepared and tested for their absorbance values using a spectrophotometer. The photothermal conversion test of BP involves low-temperature ultrasonic treatment and concentration dilution of the prepared solution, followed by temperature measurement using a femtosecond laser. The position of the quartz cuvette is adjusted, and the temperature of the BP solution under laser illumination is recorded at different time intervals until there is no significant temperature rise, indicating completion of the data measurement (Zhai et al., 2018; Jin et al., 2019). A blank control group only containing deionized water is used to ensure experimental consistency. Repeated temperature

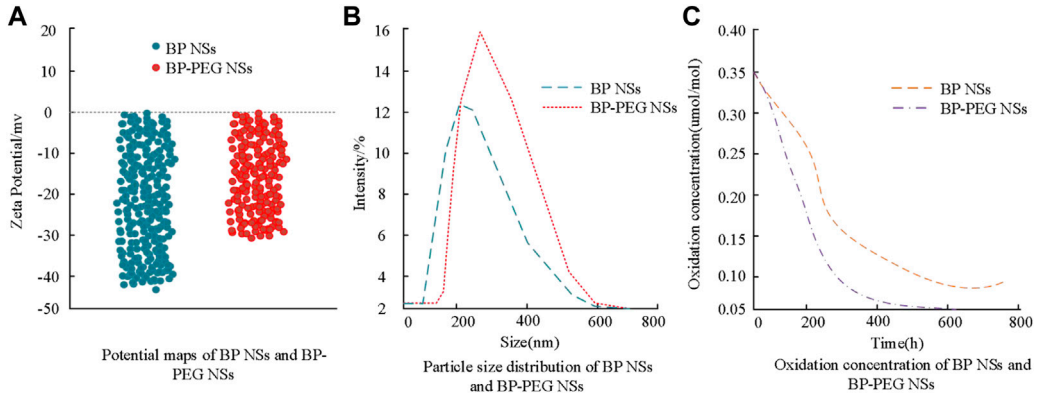


FIGURE 2
Potential map and particle size distribution of modified BP nanosheets.

measurements of the test data can provide stability analysis of the solution. The same photothermal test is carried out for PEG-modified BP as for BP.

Drug loading and release testing of BP nanomedicine: BP nanoparticles can be obtained in different particle sizes by varying experimental parameters after liquid-phase exfoliation. In this study, doxorubicin hydrochloride (DOX), a commonly used anti-tumor drug, was loaded onto BP nanosheets for nanomedicine preparation. DOX can inhibit tumor cell DNA nucleic acid synthesis and achieve killing effect on tumor cells in different stages of the cell cycle. However, it has toxic side effects such as cardiotoxicity and bone marrow suppression in clinical use (Huang et al., 2019a; Hu et al., 2019). The drug loading test is conducted as follows: 10 mL of BP is mixed with DOX and placed in a 20 ml glass bottle. The glass bottles are numbered from 1 to 4 according to their concentration ratios, with the BP solution concentration being 50 μg/mL for all four bottles and the DOX solution concentrations being 50 μg/mL, 100 μg/mL, 150 μg/mL, and 200 μg/mL, respectively. After thorough mixing, the mixed solution is subjected to centrifugation to remove excess DOX, followed by washing with deionized water to remove impurities. The extinction spectra of the DOX-containing solution and the treated DOX solution need to be recorded using a spectrophotometer at 480 nm and 800 nm to calculate the drug loading of BP at different concentration ratios. For drug release testing, the DOX-loaded BP is divided equally and placed in phosphate buffer with pH 7.5 and buffer solution with pH 5 for observation. The buffer solution with pH 5 is obtained by mixing a 0.1 M and 0.2 M solution of sodium citrate and disodium hydrogen phosphate. The corresponding dialysis bag is immersed in the corresponding pH buffer solution for standing observation, and the sample solution is subjected to extinction spectroscopy after 2 h of the experimental interval to collect the accumulated drug release data. The drug release calculation is then carried out according to the principle of drug loading testing.

### 2.1.3 Design and performance testing of targeted BP drug carrier

Good biocompatibility and biodegradability are important guarantees for nanomedicine carriers during drug delivery. BP has a specific layered two-dimensional structure and its atomic construction is highly compatible with human tissue, thus ensuring a certain level of safety. Targeted drug delivery is an effective drug delivery system that can improve the specificity of drug treatment on tumor cells and reduce damage to normal cells. PTK7 (N-term) peptide recombinant protein (PTK7) is overexpressed on the acute T-cell leukemia cell line (CCRF-CEM cells), and the heterogeneity and antigen drift of tumor cells make it difficult to label and track tumor cells. Aptamers are short oligonucleotide chains that are artificially screened with good specificity and affinity. The Sgc8 aptamer was screened from the acute leukemia tumor cell line CEM cells and can recognize the PTK7 protein (Ying-Yan et al., 2021; Grant et al., 2022). Therefore, in this study, the Sgc8 aptamer is modified on the surface of BP nanosheets to allow drug release through receptor-mediated targeting.

The cell viability test is designed as follows: After co-culturing CCRF-CEM cells with BP composite particles, the CCK-8 assay is used to evaluate cell viability. CCRF-CEM cells are seeded into a 96-well plate and incubated in a cell culture chamber with a temperature of 37°C and a gas environment of carbon dioxide for 24 h. Then, BP-PEG, BP-PEG + Laser (the laser irradiation time is 30 min), BP-PEG-DOX, and BP-PEG-DOX + Laser are added to the wells at a particle concentration of 50 μg/mL. The untreated cells serve as the control group. After incubation, the CCK-8 solution is added to each well, and the plate is incubated for 4–6 h. The optical density (OD) of each well is detected using an enzyme-linked immunosorbent assay reader (Grant et al., 2022). The same method is used to measure the cell toxicity of BP nanoparticles. By calculating the OD values of each test well and blank well and taking the average value, the cell survival rate can be obtained. However, the absorbance of BP itself at 450 nm may affect the well density. To avoid experimental errors, the OD value of the corresponding control group without particles is subtracted from that of the test well with nanoparticles, and then the cell survival rate is calculated.

Sgc8 aptamer is light and mostly attached to the tube wall, and its dry film shape is easily dispersed before opening, so it needs to be centrifuged at 4,000 rpm for 1 min first. Then, add phosphate buffer solution to make a 10 μM mixture and shake it evenly to reduce the

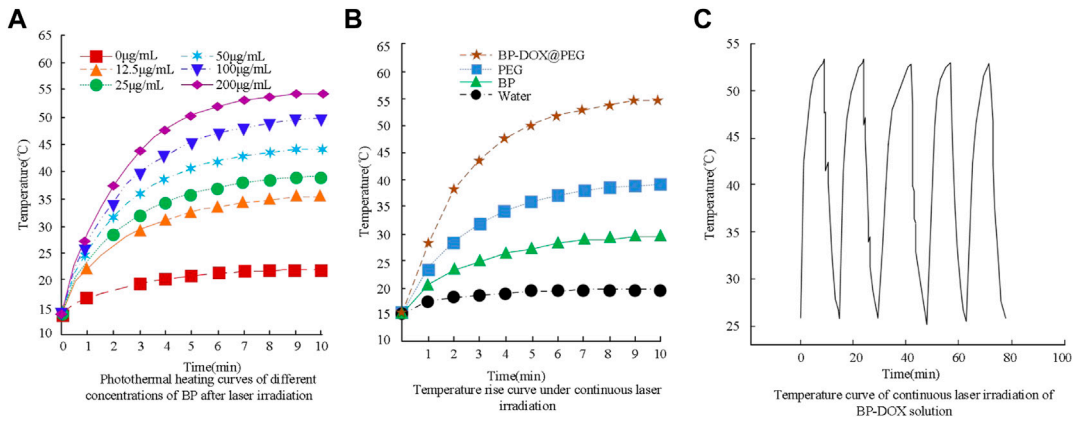


FIGURE 3
Photothermal performance of BP loaded DOX.

floating particles. Add the shaken Sgc8 aptamer to a BP-PEG solution with a concentration of 100 μg/mL, and mix it with a suitable amount of carbodiimide hydrochloride and N-hydroxysuccinimide for the activation of carboxy groups in the aptamer and the catalysis of amine groups in PEG. Lastly, after centrifuging the mixed solution at 7,800 rpm for 20 min to obtain the upper clear liquid, the excessive impurities are washed away using deionized water, and the solution is then vacuum-sealed for storage in water to complete the connection between BP and Sgc8 aptamer (Zhou et al., 2019; Gao et al., 2021). At the same time, to analyze the photothermal toxicity of BP nanodrug carrier to acute lymphoblastic leukemia cells, fluorescence imaging was performed using staining method. Specifically, 0.5 μL of calcein was added to the cell solution, shaken and placed in the dark for 10 min, and then centrifuged at 2000 rpm for 5 min. A total of 95 μL of buffer and 5 μL of propidium iodide staining solution were respectively added. After treatment, the solution was dropped under confocal microscope, and the imaging result was observed after being placed in the dark for 5 min. When releasing drugs, the Sgc8 aptamer is modified on the surface of BP-PEG particles and DOX, an anti-cancer drug, is loaded onto them under the same environmental conditions, concentration ratio, and rotational speed as BP-PEG. The cell solution with loaded drugs is shaken and cultured in an acute lymphoblastic leukemia cell culture dish, and then different BP particles are added to observe their targeting situation by fluorescence properties of anti-cancer drugs themselves.

## 2.2 Experimental data processing

During the experiment, data analysis and significance difference analysis were performed using SPSS 22.0 statistical tool, and the experimental data were expressed in the form of mean and standard deviation. $p < 0.05$ indicates statistical significance.

$$\bar{x} = \frac{\sum_{i=1}^{n} Xi}{n} \tag{1}$$

Formula (1) shows the calculation formula for the average value $\bar{x}$ of the research sample. N is the number of samples, and $Xi$ is the sample value of the $i$th number.

$$Sx = \sqrt{\frac{\sum (xi - \bar{x})^2}{n - 1}} \tag{2}$$

Formula (2) shows the calculation expression of the standard deviation $Sx$ of the research sample

$$Dload = (C/A)^{*}100\% \tag{3}$$

Formula (3) is the formula for calculating the drug loading rate, where C represents the amount of drug loading and A represents the amount of drug added.

$$Drelease = (R/C)^{*}100\% \tag{4}$$

Formula (4) is the formula for calculating the drug release rate, where R represents the amount of drug release.

$$Cellsurvival = (JOD/BOD)^{*}100\% \tag{5}$$

Formula (5) is the formula for calculating cell survival rate, where $JOD$ represents the OD value of cells with added drugs, and $BOD$ represents the OD value of cells without added drugs.

# 3 Result analysis and discussion

## 3.1 Photothermal properties of BP

The morphology of the prepared BP was analyzed using transmission electron microscopy. This microscope can present the tested sample at multiple angles, forming images with different degrees of brightness and darkness. The characterization results are shown in Figure 1.

Figure 1A shows the microscopic imaging result of BP, where it can be seen that BP forms a relatively thin layered structure. Figure 1B shows the extinction spectrum of BP. From the results, it can be seen that BP has high spectral absorption ability at different

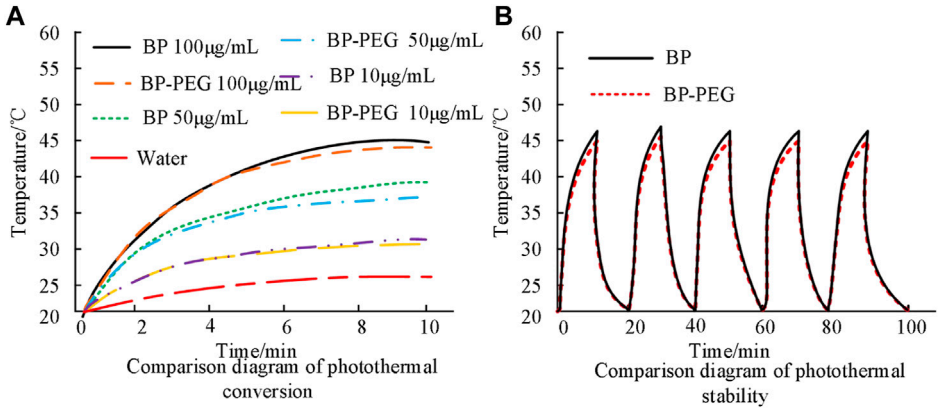


FIGURE 4
Photothermal performance and stability results under BP PEG laser irradiation.

concentrations, and the absorption ability is positively correlated with BP concentration. The maximum absorbance at a concentration of 100 μg/mL is 1.38. Figure 1C shows the results of energy spectrum analysis of BP. The results indicate that BP after being washed with deionized water contains fewer impurities and has higher purity. The above results can be used for subsequent experiments. Subsequently, the characterization of the electrochemical properties of PEG-modified BP was analyzed, and the results are shown in Figure 2.

The experimental results show that the negative potential exhibited by PEG-modified BP has increased, and the value has changed from −41.28 to −29.64, indicating an improvement in the negative potential of BP itself. Figure 2B shows the change in particle size of BP before and after modification, and it can be seen from the figure that the maximum increase in particle size is 3.55 nm. Figure 2C shows that the modified BP has good solubility and PEG can effectively alleviate the oxidation of BP. The above results indicate that the experimental design for PEG modification was successful. The photothermal properties of BP loaded with DOX after laser irradiation were analyzed, and the results are shown in Figure 3.

The temperature changes of BP under laser irradiation reflect its photothermal conversion efficiency. From the results, it can be seen that when the initial temperature of a 100 μg/mL solution is 15°C, the temperatures of the BP solution under laser irradiation for 3, 6, and 9 min are 43.6°C, 52.1°C, and 54.3°C, respectively. The increase in temperature is more pronounced with increasing concentration and photothermal conversion efficiency. In Figure 3B, the temperature rise of BP-DOX modified with polyethylene glycol PEG reached 43.7°C, 52.4°C, and 54.6°C within 3 min, 6 min, and 9 min, respectively. The temperature of the blank aqueous solution group without any solution added only increased by 3°C within 10 min. In Figure 3C, the temperature variation of BP under repeated laser irradiation was small, indicating good photothermal stability. The results of photothermal conversion of BP-PEG at different concentrations are shown in Figure 4.

In Figure 4, BP-PEG shows a significant temperature increase in a short time after laser irradiation, and the temperature increase is proportional to the concentration of BP. The temperature increase of BP-PEG solution at 100 μg/mL, 50 μg/mL, and 10 μg/mL reached 44.6°C, 36.8°C, and 29.7°C, respectively, after 10 min of NIR laser irradiation. The difference in results compared to the previous figure may be due to the absorption of NIR light by PEG. However, the values still have good photothermal efficiency compared to the water solution.

## 3.2 Analysis of drug loading characteristics of nanocarriers

A curve relationship between DOX concentration and absorbance can be established, as shown in Figure 5, with DOX concentration as the horizontal axis and absorbance as the vertical axis. The curve equation in Figure 5 is y = 18.384x+0.0398 (R2 = 0.9969). This curve can be used to analyze the drug loading and release of anti-tumor drugs. In Figure 5B, the nanoparticles have different drug release rates at different pH values. Specifically, the maximum drug release rates are 22.67% and 18.69% at pH 5 and pH 7.5, respectively. BP nanoparticles have good pH-responsive properties and can exhibit therapeutic effects in a slightly acidic environment.

Subsequently, the drug loading and drug release characteristics of BP nanoparticles were analyzed when loaded with anti-tumor drugs, and the results are shown in Figure 6.

The results in Figure 6 show that the drug loading rate of BP-DOX varies at different concentration ratios. Specifically, the increase in the anti-tumor drug DOX content led to a decrease in the drug loading rate of BP, and the values changed from 24.89% to 18.12%, and 16.23%, respectively. When the concentration difference doubled, the decreasing trend of the drug loading rate of BP became more obvious, and the rate decreased to 16.23%. In the above results, the increase of antineoplastic DOX content led to the decrease of drug loading rate of BP because black phosphorus itself has good pH trigger release characteristics, and after being modified by polyethylene glycol, it can adhere to the surface of black phosphorus, but the loading of too many

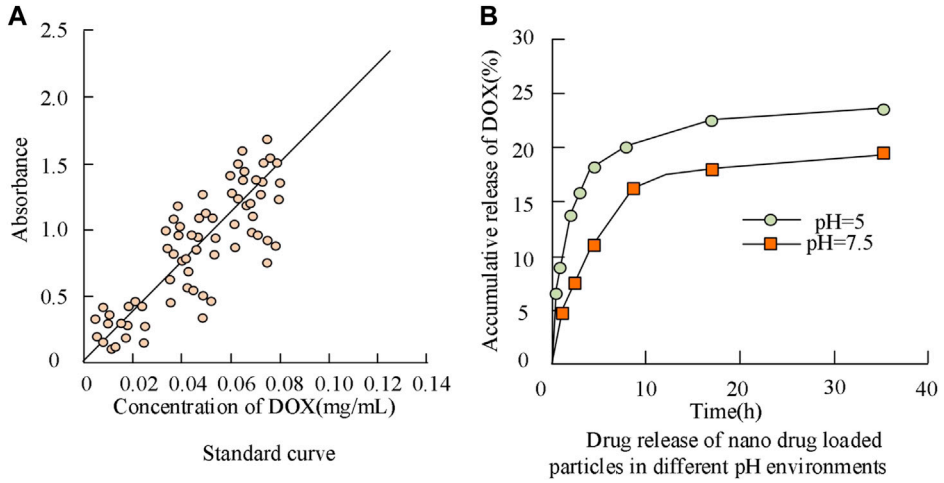


FIGURE 5
Environmental analysis of nano drug loading characteristics.

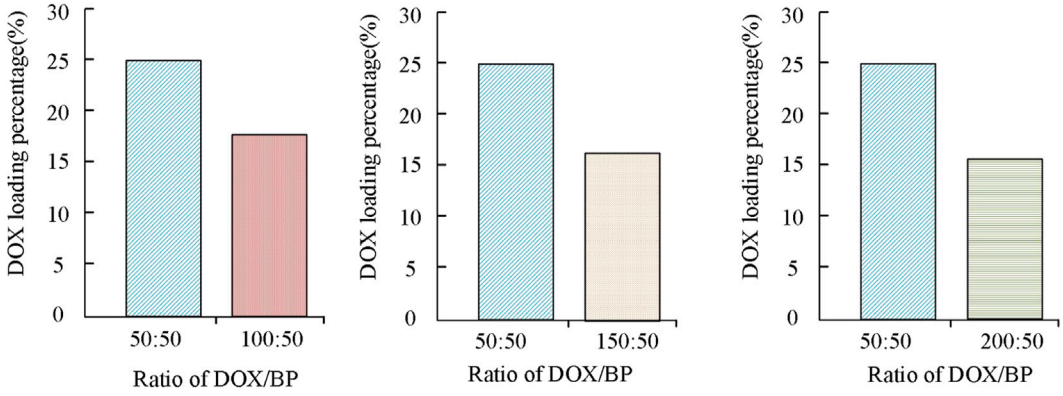


FIGURE 6
Drug loading under different DOX/BP ratios.

DOX drugs exceeded the loading capacity of nanoparticles, so it may occur drug shedding during the immersion process, thus affecting the adsorption effect of DOX and reducing the drug loading rate. The above results indicate that the ratio of anti-tumor drug to BP particles should be 1:1 for better drug loading efficiency (24.89%). The release of drugs with a higher loading rate at the ratio of 100 μg/mL:100 μg/mL under different pH value environments was analyzed, and the results are shown in Figure 7.

The results in Figure 7 show that the drug release curves of unmodified BP nanoparticles in two concentration environments exhibit an upward trend, with relatively fast initial release efficiency and gradually stabilizing in the later stage. The maximum drug release rate of BP-DOX does not exceed 10% at pH 7.5 and does not exceed 30% at pH 5. BP-PEG-DOX, after modification, has significantly higher drug release efficiency than unmodified BP-DOX in both pH environments. At pH 5, the drug loading rates at 5 h, 10 h, and 25 h of release time were 7.63%, 8.54%, and 12.13%, respectively, and at pH 7.5, the drug loading rates at 5 h, 10 h, and 25 h of release time were 17.21%, 24.89%, and 29.46%, respectively. The above results indicate that the BP nanoparticle drug carrier modified with PEG has better drug release ability. The metabolic rate of tumor cells is faster than that of normal tissues, so they produce more acid during a large amount of anaerobic respiration, which makes them appear acidic. However, if the pH is 7.5, it is closer to the human environment. Therefore, the drug release rate at pH 5 is higher than that at pH 7.5. The reason is that pH 5 neutralizes the acid-base environment in the human body, making it easier to release, thus exhibiting good release performance. At pH 7.5, the modified drug loaded nanoparticles are close to the pH value of the human body environment, which indicates that the modified materials will inhibit the release of DOX, thereby reducing the cumulative release of drugs. The modification of PEG will form an inclusion on the surface of BP nanoparticles, which will affect

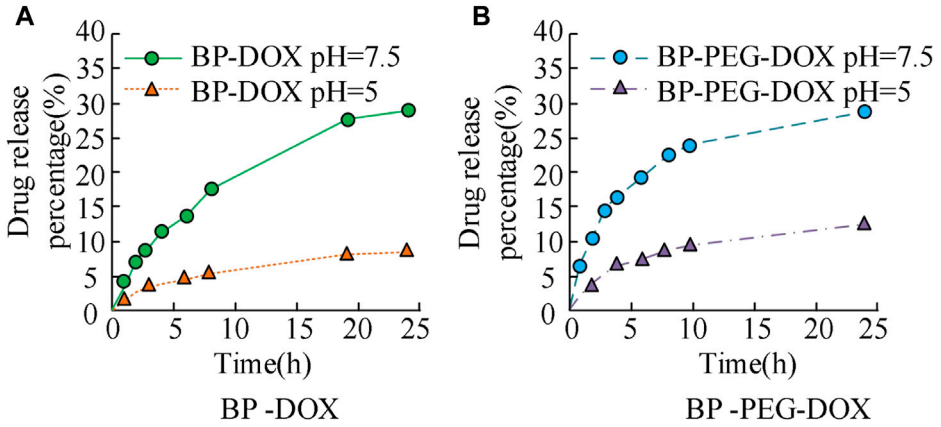


FIGURE 7
Drug release of BP drug loaded particles before and after PEG modification in different pH environments.

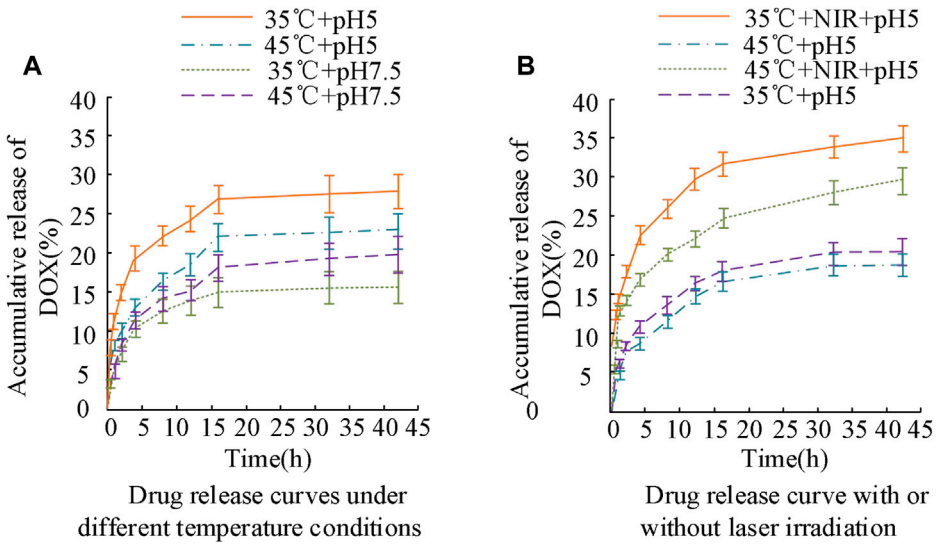


FIGURE 8
Changes in drug release curves of BP-PEG-DOX under different temperature conditions and laser irradiation.

their drug loading properties, including drug release and drug control. Subsequently, the drug release characteristics of the modified BP-PEG-DOX at different temperature conditions and under laser irradiation were further analyzed, and the results are shown in Figure 8.

The results in Figure 8A show that under different temperature conditions and laser irradiation, the drug release curves of BP-PEG-DOX exhibit different characteristics. Specifically, in the early stage of drug release (less than 15 h), the maximum drug release rate of the drug-loaded particles at pH values of 5 and 7.5 at 35°C was 24.32% and 14.87%, respectively, and their upward change curves were obvious. Later in the experiment, the drug release rates of BP-PEG-DOX reached 26.34% and 15.12%. When the temperature was 45°C, the drug release of the carrier drug was significantly lower than that under the same conditions. However, overall, the drug release of BP nanocarriers was better at pH 5°C and 35°C. In the results of Figure 8B, the drug release of BP-PEG-DOX after laser irradiation was greatly improved, and the maximum drug release rates at 35°C and 45°C reached 33.23% and 28.67%, respectively. The difference in maximum drug release rates between irradiation and non-irradiation conditions was 15.89% and 10.55%, respectively. The above results indicate that BP nanocarriers exhibit good drug release performance under laser irradiation. Moreover, there was a significant difference in drug release efficiency between Figures 8A, B. Therefore, under temperature settings and laser irradiation, BP-PEG-DOX's drug release is greatly improved, indicating the good

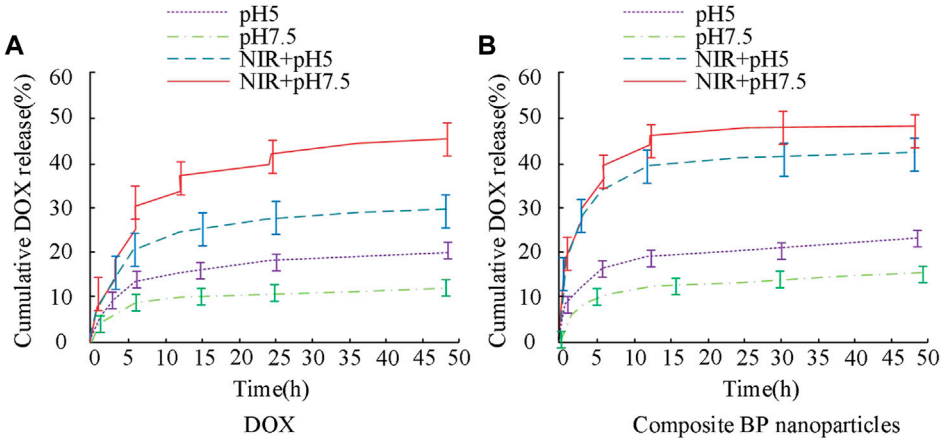


FIGURE 9
*In vitro* drug release of dual carrier BP particles.

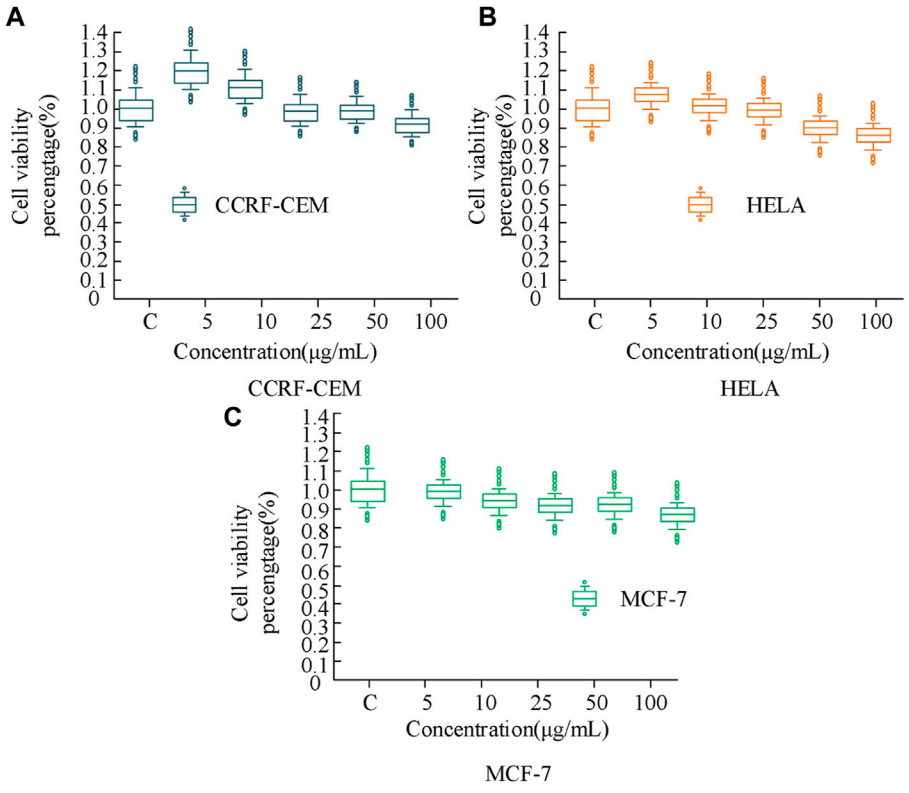


FIGURE 10
Survival of BP nanoparticles on three kinds of cells.

application efficacy of BP nanoparticles in photothermal cancer therapy. The drug release behavior of the BP dual-loading particles was analyzed in Figure 9.

Subfigures in Figure 9 represent the drug release of DOX and composite BP nanoparticles. The results show that both the single-layer and composite structures of the BP nanoparticles can maintain a good drug release rate, showing an increasing trend, and with different increment rates under different pH conditions. An acidic environment induces BP degradation, which further enables the release of internal drugs. Laser irradiation increases local temperature and accelerates the release process of BP particles. Combining the results from Figures 8, 9, it can be concluded that BP nanoparticles have good pH-responsive and photothermal properties, leading to good efficacy in tumor therapy.

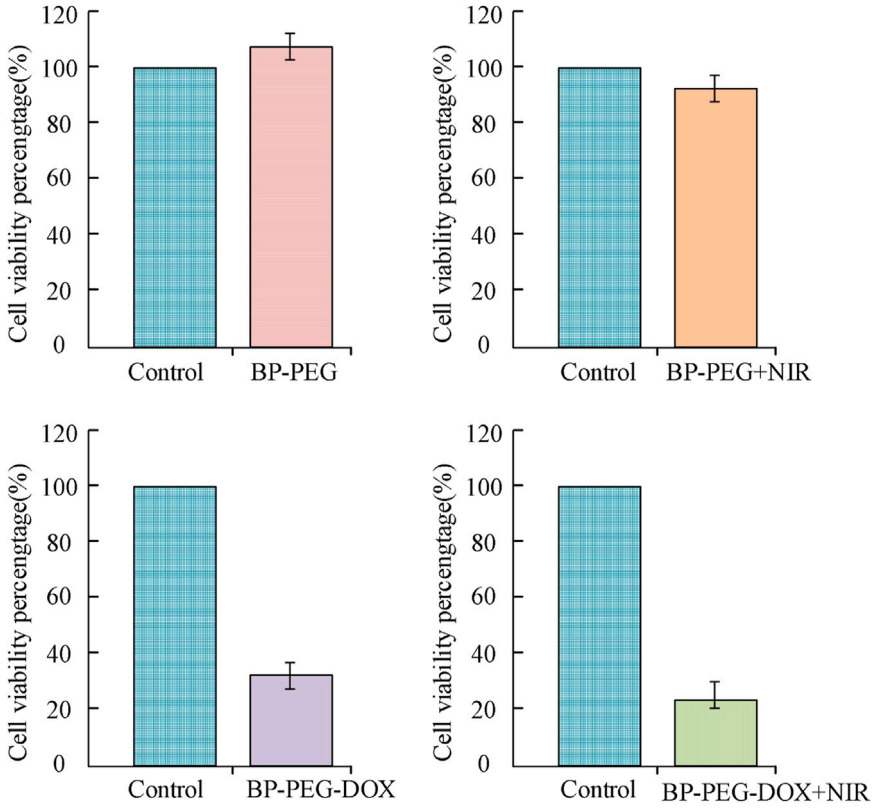


FIGURE 11
Survival of CRF-CEM cells after different treatments.

Photothermal induction can enhance the specific treatment of BP particles for tumor parts.

## 3.3 Analysis of the targeted therapeutic effect of nanocarriers in leukemia

Targeted therapy is a means of drug therapy at the cellular and molecular level for cancer sites, in which the drug interacts specifically with the cancer site, leading to cell apoptosis, and will not cause damage to other normal cells. The study analyzed the targeted therapeutic effect of BP nanocarriers in leukemia, and analyzed the cell survival status. The results are shown in Figure 10.

In Figure 10, the horizontal and vertical axes represent the cell survival status of BP-PEG nanoparticles and the blank control group, respectively. The results show that the influence of the drug carrier form on cell survival status varies at different concentrations. Specifically, when the particle concentration was 5 μg/mL, the survival rates of the three cells (CCRF-CEM, HELA, MCF-7) were 120.18%, 109.89%, and 100.21%, respectively; when the particle concentration was 25 μg/mL, their survival rates were 101.36%, 100.17%, and 92.13%, respectively; and when the particle concentration was 100 μg/mL, their survival rates were 96.24%, 89.23%, and 89.23%, respectively. The above results indicate that when the BP concentration is low, its effect on cell proliferation is not obvious. With the increase of particle concentration, the toxic side effects of BP on cancer cells are low, and the cells overall remain more than 85% alive, indicating that BP nanoparticles have a high level of drug safety. The photothermal toxicity of the BP drug carrier was analyzed, and its results were analyzed using a cell proliferation test kit, as shown in Figure 11.

The results in Figure 11 show that compared with the control group, the survival rates of BP particles after PEG modification, laser treatment, attachment of antitumor drug carriers, and "modification + laser treatment" were 105.89%, 88.94%, 32.01%, and 18.79%, respectively. Specifically, the BP-PEG-DOX nanoparticles modified by PEG and the BP-PEG + NIR treated by laser have a significant killing effect on cells, with their cell survival rates decreasing by 73.88% and 16.95%, respectively. This result indicates that the modification and laser treatment of BP particles can effectively inhibit the growth of cancer cells. Moreover, the cell survival rate of BP-PEG-DOX + NIR after "modification + laser treatment" decreased most significantly, indicating that BP has a good intervention effect in photothermal therapy. The staining results of cancer cells treated with BP particles are analyzed in Figure 12.

In Figure 12, the red part represents the apoptotic cells. The results show that after cancer cells were cultured with BP particles, the nanoparticles have a significant apoptotic effect on cancer cells, and the number of apoptotic cells is significantly higher than that

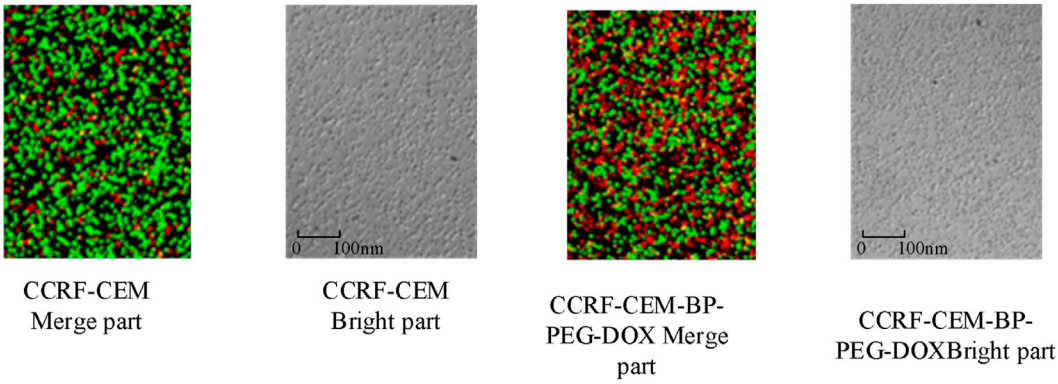


FIGURE 12
Dye fluorescence imaging results of anti-tumor cells treated with BP nanoparticles.

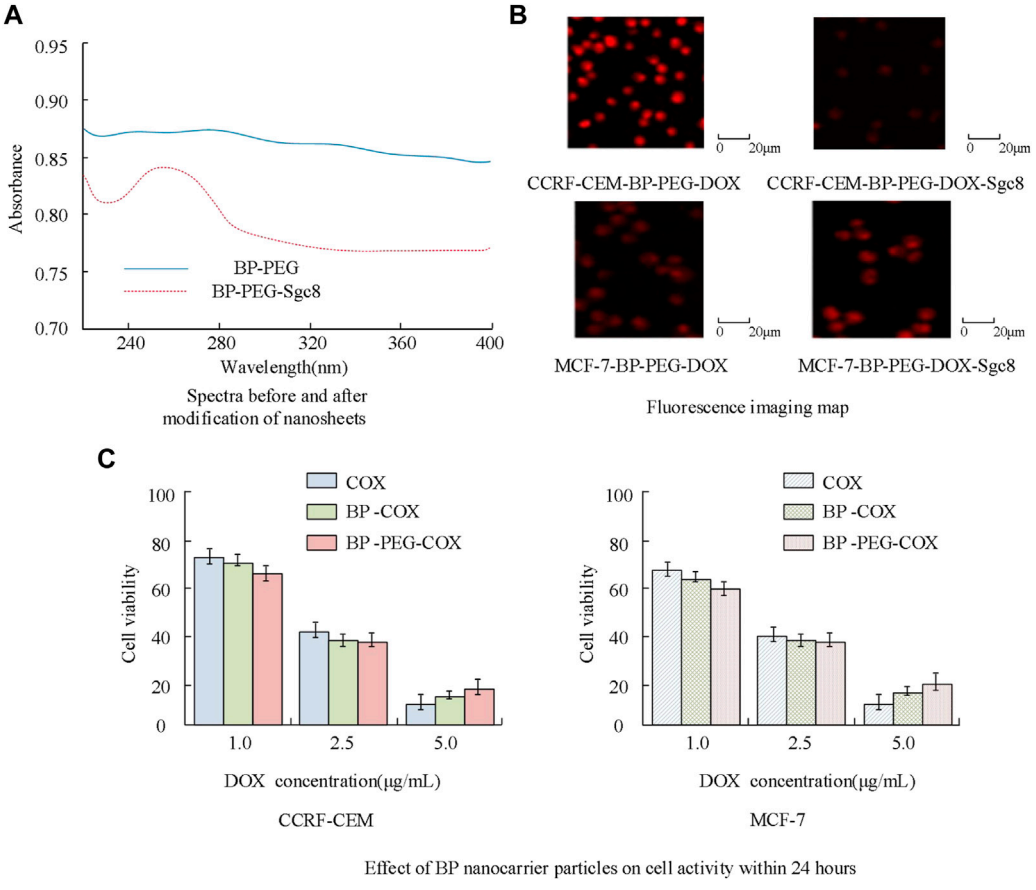


FIGURE 13
Effects of Sgc8 aptamer on two types of cells.

without nanocarrier drugs. Subsequently, the BP nanocarrier was analyzed for cancer cell expression. Acute lymphoblastic leukemia cells surface express PTK7 abundantly, and they can identify Sgc8 aptamer well, so breast cancer cells (MCF-7) and leukemia cells were compared for better analysis of BP nanoparticle drug release. The results are shown in Figure 13.

In Figure 13A, there is a peak at 265 nm before and after the aptamer modification of BP nanoparticles, which can effectively

achieve the modification of nanoparticles and their surface connection. In Figure 13B, the fluorescence intensity of CCRF-CEM cells is significantly higher than that of co-cultured particle drug carriers and higher than that of co-cultured MCF-7 cells, and the fluorescence intensity of cells under Sgc8 receptor intervention changes less. The above results indicate that BP nanoparticles can achieve targeted therapy for leukemia cells, improve the internalization of particles, and have a good intervention effect. The reason is that the strong chelating ability of the polyethylene glycol modified BP nanoparticle under phosphorus oxide is improved, effectively improving the stability of BP. The addition of aptamers will increase the phosphorus oxide current including phosphite ions on BP, thereby enhancing its signal ability and sensitivity in biological detection. At the same time, the aptamer has a small molecular weight, high tissue permeability, and is easy to modify with drugs. Its combination with BP nanoparticles can effectively reverse the activity of aptamer, relieve the inhibition of tumor cells, and have good biological stability after PEG modification. The antitumor drug has a significant inhibitory effect on the growth of breast cancer cells, and the analysis of drug loading using BP nanoparticles can effectively reduce cell toxicity. The reason is that DOX has strong cell toxicity and limited residual effects in the body, while BP nanocarriers can improve the selectivity of chemotherapeutic drugs, thereby reducing their toxic side effects.

## 4 Conclusion

The application of nano drug delivery systems provides new research value for the treatment of medical tumors. The research is based on the characteristics of black phosphorus two-dimensional nanoparticles for preparation, drug loading characteristics and targeted treatment analysis in leukemia. The results indicate that polyethylene glycol modified BP can effectively improve the negative charge situation, and the temperature rise of BP-DOX is significantly higher than that of the blank aqueous solution group, indicating good photothermal conversion efficiency. The increase in anti-tumor drug DOX resulted in a decrease in the drug loading of BP, with values increasing from 24.89% to 18.12% and 16.23%, respectively. The maximum drug release rates at pH values of 7.5 and 5 shall not exceed 10% and 30%. The drug release efficiency of modified BP-PEG-DOX was significantly higher than that of unmodified BP-DOX in two pH environments. And the release curve of BP-PEG-DOX is in the early stage, with a maximum release rate of 24.32% at a temperature of 35°C and a pH value of 5. The maximum drug release rates of BP-PEG-DOX-NIR reached 33.23% and 28.67% at temperatures of 35°C and 45°C, with corresponding values of 15.89% and 10.55% difference compared to those without laser irradiation. Moreover, the cell survival rates of BP-PEG-DOX and BP-PEG + NIR decreased by 73.88% and 16.95%, indicating significant cell killing effects. The composite BP particles have good drug release properties, and they have good drug induction specificity and drug loading properties under photothermal conditions. In photodynamic therapy, photosensitizers generate cytotoxic intracellular ROS through photochemical reactions, which is a non-invasive treatment mode. Zong, SF scholars proposed modifying the prepared BPNS with polyethylene glycol (PEG) and applying it in the synergistic targeted photothermal therapy of acute lymphoblastic leukemia (ALL). The results indicate that, BPNS@PEG the nanoparticles modified with Sgc8 aptamer showed good specificity and endocytosis for CCRF-CEM cells (Zong et al., 2019b). BP nanocarrier particles can reduce toxicity and side effects in targeted therapy of leukemia cells, and have broad application value in the field of tumor therapy (Huang et al., 2019b).

## Data availability statement

The original contributions presented in the study are included in the article/supplementary material, further inquiries can be directed to the corresponding author.

## Author contributions

Conceptualization, YY; Supervision, YY; Validation, XL; Visualization, ZZ; Writing-original draft, YY; Writing-review and editing, YY. All authors contributed to the article and approved the submitted version.

## Conflict of interest

The authors declare that the research was conducted in the absence of any commercial or financial relationships that could be construed as a potential conflict of interest.

## Publisher's note

All claims expressed in this article are solely those of the authors and do not necessarily represent those of their affiliated organizations, or those of the publisher, the editors and the reviewers. Any product that may be evaluated in this article, or claim that may be made by its manufacturer, is not guaranteed or endorsed by the publisher.

## References

Cai, X., Xie, Z., and Ding, B. (2019). Monodispersed copper (I)-Based nano metal–organic framework as a biodegradable drug carrier with enhanced photodynamic therapy efficacy. *Adv. Sci.* 6 (15), 1900848.

Dadwal, A., Baldi, A., and Kumar Narang, R. (2018). Nanoparticles as carriers for drug delivery in cancer. *Artif. cells, nanomedicine, Biotechnol.* 46 (2), 295–305.

Duarte, Y., Marquez-Miranda, V., Miossec, M. J., and Gonzalez-Nilo, F. (2019). Integration of target discovery, drug discovery and drug delivery: A review on computational strategies. *Wiley interdiscip. Reviews-nanomedicine nanobiotechnology* 11 (4), 1939–5116.

El-Boubbou, K. (2018). Magnetic iron oxide nanoparticles as drug carriers: Clinical relevance. *Nanomedicine* 13 (8), 953–971.

El-Boubbou, K. (2018). Magnetic iron oxide nanoparticles as drug carriers: Preparation, conjugation and delivery. *Nanomedicine* 13 (8), 929–952.

Gao, S., Yang, X., and Xu, J. (2021). Nanotechnology for boosting cancer immunotherapy and remodeling tumor microenvironment: The horizons in cancer treatment. *ACS Nano* 15 (8), 12567–12603.

Grant, C. V., Russart, K., and Pyter, L. M. (2022). A novel targeted approach to delineate a role for estrogen receptor-beta in ameliorating murine mammary tumor-associated neuroinflammation. *Endocrine* 75 (3), 949–958.

Guo, L., and Chen, H. (2018). Effects of surface modifications on the physicochemical properties of iron oxide nanoparticles and their performance as anticancer drug carriers. *Chin. Chem. Lett.* 29 (12), 1829–1833.

Herrmann, I. K., Wood, M. J. A., and Fuhrmann, G. (2021). Extracellular vesicles as a next-generation drug delivery platform. *Nat. Nanotechnol.* 16 (7), 748–759.

Hu, T., Mei, X., and Wang, Y. (2019). Two-dimensional nanomaterials: Fascinating materials in biomedical field. *Sci. Bull.* 64 (22), 1707–1727.

Huang, H., Dong, Y., and Zhang, Y. (2019). GSH-sensitive Pt(IV) prodrug-loaded phase-transitional nanoparticles with a hybrid lipid-polymer shell for precise theranostics against ovarian cancer. *Theranostics* 9 (4), 1047–1065.

Huang, X., Wu, B., and Li, J. (2019). Anti-tumour effects of red blood cell membrane-camouflaged black phosphorous quantum dots combined with chemotherapy and anti-inflammatory therapy. *Artif. Cells, Nanomedicine, Biotechnol.* 47 (1), 968–979.

Jin, A., Wang, Y., and Lin, K. (2020). Nanoparticles modified by polydopamine: Working as "drug" carriers. *Bioact. Mater.* 5 (3), 522–541.

Jin, S., Du, Z., and Guo, H. (2019). Novel targeted anti-tumor nanoparticles developed from folic acid-modified 2-deoxyglucose. *Int. J. Mol. Sci.* 20 (3), 697–708.

Kimura, N., Maeki, M., and Sato, Y. (2018). Development of the iLiNP device: Fine tuning the lipid nanoparticle size within 10 nm for drug delivery. *ACS omega* 3 (5), 5044–5051.

Kong, N., Ji, X., and Wang, J. (2020). ROS-Mediated selective killing effect of black phosphorus: Mechanistic understanding and its guidance for safe biomedical applications. *Nano Lett.* 20 (5), 3943–3955.

Li, C., Wang, J., and Wang, Y. (2019). Recent progress in drug delivery. *Acta Pharm. sin. B* 9 (6), 1145–1162.

Liu, C., Shin, J., and Son, S. (2021). Pnictogens in medicinal chemistry: Evolution from erstwhile drugs to emerging layered photonic nanomedicine. *Chem. Soc. Rev.* 50 (4), 2260–2279.

Liu, Y. L., Chen, D., and Shang, P. (2019). A review of magnet systems for targeted drug delivery. *J. Control. Release* 302, 90–104.

Medina-Sánchez, M., Xu, H., and Schmidt, O. G. (2018). Micro-and nano-motors: The new generation of drug carriers. *Ther. Deliv.* 9 (4), 303–316.

Moller, K., and Bein, T. (2019). Degradable drug carriers: Vanishing mesoporous silica nanoparticles. *Chem. Mater.* 31 (12), 4364–4378.

Paknia, F., Mohabatkar, H., Ahmadi-Zeidabadi, M., and Zarrabi, A. (2022). The convergence of *in silico* approach and nanomedicine for efficient cancer treatment; *in vitro* investigations on curcumin loaded multifunctional graphene oxide nanocomposite structure. *J. DRUG Deliv. Sci. Technol.* 71, 711773–712247.

Pullan, J. E., Confeld, M. I., and Osborn, J. K. (2019). Exosomes as drug carriers for cancer therapy. *Mol. Pharm.* 16 (5), 1789–1798.

Qiu, M., Wang, D., and Liang, W. (2018). Novel concept of the smart NIR-light–controlled drug release of black phosphorus nanostructure for cancer therapy. *Proc. Natl. Acad. Sci.* 115 (3), 501–506.

Rai, V. K., Mishra, N., and Yadav, K. S. (2018). Nanoemulsion as pharmaceutical carrier for dermal and transdermal drug delivery: Formulation development, stability issues, basic considerations and applications. *J. Control. release* 270, 203–225.

Shao, X., Ding, Z., and Zhou, W. (2021). Intrinsic bioactivity of black phosphorus nanomaterials on mitotic centrosome destabilization through suppression of PLK1 kinase. *Nat. Nanotechnol.* 16 (10), 1150–1160.

Wang, C., Zhang, W., and He, Y. (2021). Ferritin-based targeted delivery of arsenic to diverse leukaemia types confers strong anti-leukaemia therapeutic effects. *Nat. Nanotechnol.* 16 (12), 1413–1423.

Ying-Yan, M., Meng, L., and Jin-Da, W. (2021). NIR-triggered drug delivery system for chemo-photothermal therapy of posterior capsule opacification. *J. Control. Release* 339, 391–402.

Zhai, Y., Zhou, X., and Zhang, Z. (2018). Design, synthesis, and characterization of schiff base bond-linked pH-responsive doxorubicin prodrug based on functionalized mPEG-PCL for targeted cancer therapy[J]. *Polymers* 10 (10), 1127–1138.

Zhang, H., Fan, T., and Chen, W. (2020). Recent advances of two-dimensional materials in smart drug delivery nano-systems. *Bioact. Mater.* 5 (4), 1071–1086.

Zhou, M., Yi, Y., and Liu, L. (2019). Polymeric micelles loading with ursolic acid enhancing anti-tumor effect on hepatocellular carcinoma. *J. Cancer* 10 (23), 5820–5831.

Zhu, Y., Liu, Y., and Xie, Z. (2021). Magnetic black phosphorus microbubbles for targeted tumor theranostics. *Nanophotonics* 10 (12), 3339–3358.

Zong, S., Wang, L., and Yang, Z. (2019). Black phosphorus-based drug nanocarrier for targeted and synergetic chemophotothermal therapy of acute lymphoblastic leukemia. *ACS Appl. Mater. interfaces* 11 (6), 5896–5902.

Zong, S. F., Wang, L. L., Yang, Z. Y., Wang, H., Wang, Z. Y., and Cui, Y. P. (2019). Black phosphorus-based drug nanocarrier for targeted and synergetic chemophotothermal therapy of acute lymphoblastic leukemia. ACS APPLIED MATERIALS and INTERFACES. *ACS Appl. Mater. INTERFACES* 11 (6), 5896–5902.